Master of Science Thesis in Electrical Engineering
Department of Electrical Engineering, Linköping University, 2018

Optimal Control of Heat Transfer Rates in Turbochargers

Max Johansson

LINKÖPING UNIVERSITY

Master of Science Thesis in Electrical Engineering

Optimal Control of Heat Transfer Rates in Turbochargers

Max Johansson

LiTH-ISY-EX--18/5157--SE

Supervisor: **Kristoffer Ekberg**
ISY, Linköping University
Oskar Leufvén
Scania CV AB

Examiner: **Lars Eriksson**
ISY, Linköping University

Division of Vehicular Systems
Department of Electrical Engineering
Linköping University
SE-581 83 Linköping, Sweden

Sammanfattning

Turboladdaren är en viktig komponent i konkurrenskraftiga miljövänliga fordon. Styrningen av turboladdare kräver modeller, som parameteriseras med hjälp av mätdata från turboprovning i *Gas Stands* (en gasflödesbänk, där fordonets motor ersätts med en brännare, så att avgaserna till turboladdaren kan styras med hög noggrannhet). Anskaffning av den medelvärdesbildade data som krävs, är en utdragen procedur, och kan ta mer än ett dygn per laddare. För att få tillräcklig noggrannhet i mätningen måste systemet nå termodynamisk jämvikt efter ett byte av arbetspunkt, vilket tar lång tid. Det är särskilt turboladdarens matrialtemperaturer som tar tid att svänga in.

En hypotes är att moderna reglertekniska metoder, som numerisk optimal styrning, drastiskt skulle kunna minska insvängningstiden vid byte av turboladdarens arbetspunkter under provning. Syftet med denna uppsats är att förse Scania med en metod för tidsoptimal provning av turboladdare.

I uppsatsen så parametersätts modeller för en turboladdare, som delas in i turbin, lagerhus och kompressor. Relativt enkla modeller används för att beskriva värmeflödet från avgaser och laddluft, till turbons material, och interna värmeflöden inuti laddaren. De separata modellerna, både mekaniska och termodynamiska, slås ihop till en komplett modell för turboladdaren. Modellen valideras mot data från uppmätta stegsvar.

Numerisk optimal styrning används för att beräkna optimala trajektorier för turboladdarens styrsignaler, så att stationäritet nås så snabbt som möjligt, för en given arbetspunkt. *Direct collocation* är en metod som innebär att man diskretiserar det optimala styrningsproblemet, och använder en lösare för icke-linjär optimering. Resultatet visar att insvängningstiden mellan arbetspunkter kan förkortas med en faktor på 23.

När optimal förflyttning mellan arbetspunkter är möjligt, så undersöks om mer vinster kan hämtas genom att hitta en optimal sekvens av förflyttningar genom mappen. Problemet är ett öppet handelsresandeproblem, vilka är väl studerade, och en optimal lösning inte kan garanteras. En nära optimal väg hittas genom att använda en genetisk algoritm. Resultatet visar att en optimal väg inte ger mycket mer förbättring än den metod som mappen är uppmätt med från början.

Den utvecklade metoden kräver en modell för att beräkna styrsignalerna. Provningen görs för att få data, så att en modell kan skapas, en moment-22-situation. Det kan undvikas genom att använda systemidentifiering. Under gas standets uppvärmingsperiod, kan stegsvar utföras och de modellparametrar som är nödvändiga för styrningen estimeras, utan tidigare kunskap om turboladdaren.

Abstract

The turbocharger is an important component of competitive environmentally friendly vehicles. Mathematical models are needed for controlling turbochargers in modern vehicles. The models are parameterized using data, gathered from turbocharger testing in *gas stands* (a flow bench for turbocharger, where the engine is replaced with a combustion chamber, so that the exhaust gases going to the turbocharger can be controlled with high accuracy). Collecting the necessary time averaged data is a time consuming process. It can take more than 24 hours per turbocharger. To achieve a sufficient level of accuracy in the measurements, it is required to let the turbocharger system reach steady state after a change of operating point. The turbocharger material temperatures are especially slow to reach steady state.

A hypothesis is that modern methods in control theory, such as numeric optimal control, can drastically reduce the wait time when changing operating point. The purpose of this thesis is to provide a method of time optimal testing of turbochargers.

Models for the turbine, bearing house and compressor are parameterized. Well known models for heat transfer is used to describe the heat flows to and from exhaust gas and charge air, and turbocharger material, as well as internal energy flows between the turbocharger components. The models, mechanical and thermodynamic, are joined to form a complete turbocharger model, which is validated against measured step responses.

Numeric optimal control is used to calculate optimal trajectories for the turbocharger input signals, so that steady state is reached as quickly as possible, for a given operating point. *Direct collocation* is a method where the optimal control problem is discretized, and a non-linear program solver is used. The results show that the wait time between operating points can be reduced by a factor of 23.

When optimal trajectories between operating points can be found, the possibility of further gains, if finding an optimal sequence of trajectories, are investigated. The problem is equivalent to the open traveling salesman, a well studied problem, where no optimal solution can be guaranteed. A near optimal solution is found using a genetic algorithm.

The developed method requires a turbocharger model to calculate input trajectories. The testing is done to acquire data, so that a model can be created, which is a catch-22 situation. It can be avoided by using system identification techniques. When the gas stand is warming up, the necessary model parameters are estimated, using no prior knowledge of the turbocharger.

Acknowledgments

I would like to give special thanks to my supervisors Kristoffer Ekberg and Oskar Leufvén, my examiner Lars Eriksson, and the division of Vehicular Systems at Linköping University, as well as NMGG at Scania, without which this project would not have been possible.

I would like to thank my family and friends, especially the bees, for these five years of fun.

Linköping, June 2018
Max Johansson

Contents

Notation

Notation	Meaning
T	Temperature $[K]$
p	Pressure $[Pa]$
m	Mass $[kg]$
$\dot{m}$	Mass flow $[kg/s]$
Π	Pressure ratio [-]
ω	Rotational speed $[rad/s]$
r	Radius $[m]$
c_p	Heat capacity at constant pressure $[J/(kg\ K)]$
c_v	Heat capacity at constant volume $[J/(kg\ K)]$
γ	Heat capacity ratio [-]
η	Efficiency [-]
ρ	Density $[kg/m^3]$
D	Diameter $[m]$
R	Ideal gas constant $[J/(kg\ K))$
V	Volume $[m^3]$
T_q	Torque $[N\,m]$
μ	Dynamic viscosity $[kg/(m\ s)]$
J	Inertia $[kg\ m^2]$
A	Area $[m^2]$
Pr	Prandtl's Number [-]
λ	Thermal conductivity $[W/(m\ K)]$
$\dot{Q}$	Heat transfer $[W]$

Abbreviation	Meaning
OCP	Optimal Control Problem
NLP	Non-Linear Program
IPOPT	Interior Point OPTimizer

1 Introduction

1.1 Purpose and Goals

A project has been running which aims to supply Scania with in house turbocharger testing capabilities, and is now in its final stage. The result of this project is a turbocharger test bed, referred to as a *gas stand*, and is used to measure turbine and compressor properties.

The testing procedure produces turbocharger *maps*, in essence a relation between mass flow-pressure ratio, and mass flow-efficiency, for varying turbocharger speeds. The maps are used to model the turbocharger, and the accuracy of the maps affect its performance when the models are used in an engine control system. A potential source of error is that the measurements are made without letting certain temperatures reach steady state. However, due to the thermal inertia of the system, reaching steady state takes a considerable amount of time under normal conditions.

The first goal of this master thesis project is to develop control strategies, that minimize the time it takes for the system to reach steady state, when switching between turbocharger operating points. The second goal is to find the optimal path through a set of target operating points, so that a complete compressor or turbine map can be made as quickly as possible. Optimal control and turbocharger heat transfer, separately, are wide and active fields of research. Combining the two and applying it to gas stands is new, which is what makes this project worthwhile.

1.2 Related Research

Turbochargers play an important role in fuel efficient vehicles. The design and optimization of turbocharger configurations relies on the availability of high quality data. The data is usually represented in a turbocharger map according to standardized procedures, given by e.g. SAE and ASME ASME (1997), SAE (1995a,b). The acquisition of the turbocharger maps can be time consuming, since it is necessary to wait until thermal equilibrium is reached for the turbocharger before the measurement data can be acquired and averaged. As an example the well populated map, Figure 7, in Eriksson (2007), containing 91 points, took 34 hours to measure in a gas stand at a subcontractor.

An early design of a gas stand was proposed by Young and Penz (1990), and later by Venson et al. (2006). Despite the years of study, no efforts have yet been made to directly counter what is now a major bottleneck in turbocharger testing, the thermal inertia. And as environmental legislation becomes stricter, the demand for accuracy in turbocharger maps will increase. This puts pressure on the engine testing industry to adapt modern control methods to improve testing.

One modern method, that is gaining attention and traction, is numerical optimal control. Its advantage lies in its ability to deal with non-linear, non-convex, and large problems. In the *direct* category of numerical optimal control, the optimal control problem (OCP) is discretized to a non-linear program (NLP). An NLP solver is then used to generate optimal trajectories.

The experimental data for this thesis was gathered at SAAB's gas stand, 2011. The turbocharger used was a Mitsubishi TD04. In order to parameterize a heat transfer model, several maps was measured with different exhaust and oil temperatures. To validate a complete turbocharger model, a separate sequence of consecutive step responses were made.

A design for a turbocharger testing facility is presented by Stemler and Lawless (1997). It is a very similar design to Scania's gas stand. One difference, is that Scania has two combustion chambers, so that twin-scroll properties can be measured.

A compressor model was presented by Llamas and Eriksson (2017). Using the parameterization technique from Llamas and Eriksson (2016), a MATLAB toolbox for compressor modeling was provided in Llamas and Eriksson (2018). This toolbox can be used to efficiently parameterize compressor models, and adjust the efficiency map to correct for heat transfer. Several models of the turbocharger, such as turbine mass flow, friction etc. are collected and summarized in Eriksson and Nielsen (2014).

A simple heat transfer model, which consists of dividing the turbocharger in only three components, the compressor, turbine and bearing housing, was stud-

ied by Baines et al. (2010). This model was successfully implemented to augment an adiabatic turbocharger model by Bengtsson (2015). Complex models with more nodes are were studied by Serrano et al. (2014), and Olmeda et al. (2011). However, these models require more temperature measurements to parametrize than the simple model.

The Scania gas stand uses a long curved pipe to connect the combustion chamber to the turbine inlet. Ekberg (2015) studies the effects of non-ideal inlet pipes when making turbocharger measurements. The author concludes that heat transfer and pressure losses in the measurement setup causes the efficiency maps to differ from in-vehicle performance.

According to Asprion et al. (2014), optimal control methods such as dynamic programming, or solving the Hamilton-Jacobi-Bellman equation, are not suited for systems with a large number of states. Instead, the optimal control problem (OCP), is better solved by one of the *direct* methods. The direct methods work by discretizing the system trajectories, creating a non linear program (NLP), as described by Diehl (2011). The NLP is solved by using one of many solvers, an example being *IPOPT* (Wächter, 2013).

There are multiple helpful tools for implementation of numerical optimal control, such as *CasADi*, by Andersson (2013) and *PROPT* (TOMLAB, 2016). Leek (2016) created a toolbox for *MATLAB* was created to help engineers without experience in numerical optimization, solving OCP's. These tools combined, have been used to successfully produce optimal state and control trajectories, for systems that includes turbochargers. One example of such a study was done by Leek et al. (2017).

As stated by Sivertsson and Eriksson (2014), the models used in OCP's should handle extrapolation well, and be continuously differentiable.

1.3 System Overview and Delimitations

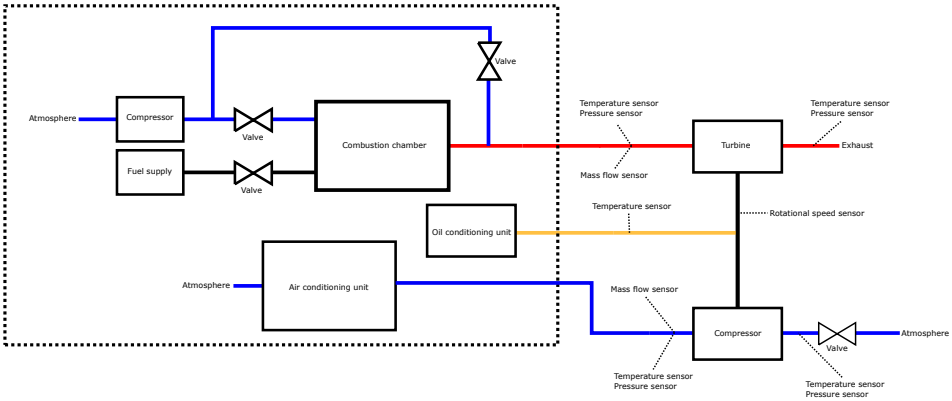

Figure 1.1: *The gas stand system overview. Components within the dashed rectangle are not modeled, and are outside the scope of this thesis project.*

Figure 1.1 shows an overview of the complete system. The gas stands works by burning fuel and compressed air in the combustion chamber, which is then expelled to the turbine inlet. The use of a burner instead of an internal combustion engine, ensures that the temperature and pressure of exhaust gases in the turbine inlet is easy to control, and removes any pressure pulsations due to the engine. An oil conditioning unit supplies the turbocharger with oil, and cools the returning oil. The air conditioning unit keeps the temperature in the room, and the air going to the compressor inlet, constant.

The compressor circuit can be constructed in two configurations, open loop and closed loop. In the closed loop compressor circuit, the charge air is led into an intercooler, and then back to the compressor inlet. This configuration avoids compressor stall for high power turbine testing. In open loop configuration, the charge air is simply let out.

The validation data for this project was gathered at Saab, in Trollhättan, 2011. The intention however, is to use this method at another gas stand. The differences in the two setups, and the time constraints on this project, makes it necessary to introduce limitations in scope.

The first limitation, is the assumption that exhaust gas temperature and pressure, are regarded as exogenous inputs, and independently controllable. This assumption removes the need to model a combustion chamber, compressor (which is used to compress the air before the combustion chamber), and a number of control valves.

Further, only the open loop case (the compressed air is not led back into the

compressor inlet) is investigated.

The turbocharger in question, the Mitsubishi TD04, is water cooled. Since the majority of Scania turbochargers are not, only oil cooling is considered in the optimal control. The water cooling is modeled, but only to provide better validation for the full model.

The heat transfer, in the pipe connecting the turbine and combustion chamber, is neglected.

2

Model and Validation

2.1 Turbocharger model

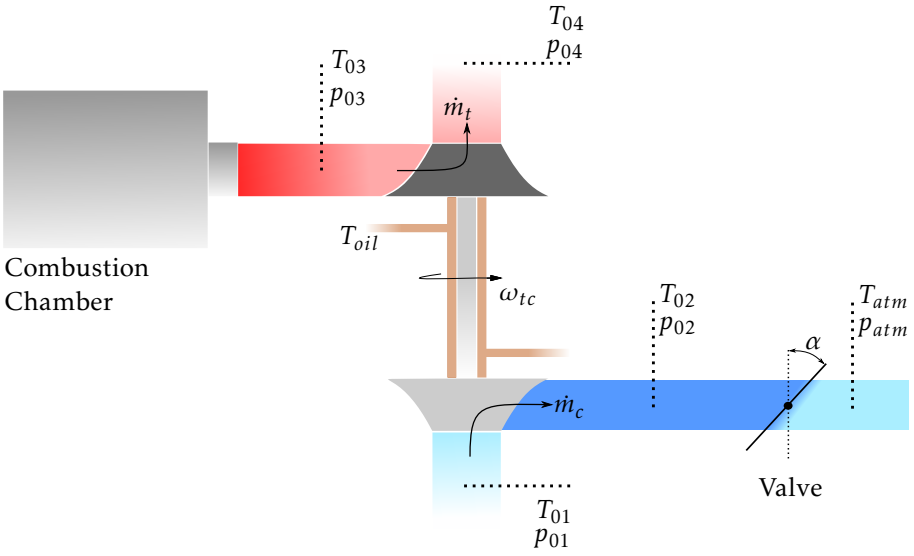

Figure 2.1: *Overview of the mechanical system. Inputs are the exogenous burner temperature and pressure, T_{03} and p_{03}, the oil temperature T_{oil}, and the valve angle α. States are the turbocharger rotational speed ω_{tc} and the charge pressure p_{02}. T_{02} is assumed constant from the compressor to the valve. The oil mass flow $\dot{m}_{oil}$, could have been used as an additional input signal, but since it would produce the same effect as changing T_{oil}, it is kept constant, for computational efficiency.*

Figure 2.1 shows the turbocharger system overview. The temperature and pressure from the gas burner are seen as exogenous inputs and are shown in the Figure. In addition to the oil circuit, the TD04 turbocharger has a water circuit for cooling. The water circuit has been modeled but is not included in the optimal control problem setting.

2.1.1 Turbine

The turbine massflow is modeled as proposed in Eriksson and Nielsen (2014).

$$\Pi_t = \frac{p_{04}}{p_{03}} \tag{2.1}$$

$$TFP = \dot{m}_t \frac{\sqrt{T_{03}}}{p_{03}} \tag{2.2}$$

$$TFP = TFP_{max} \sqrt{1 - \Pi_t^{TFP_{exp}}} \tag{2.3}$$

Where $\dot{m}_t$ is the turbine mass low, Π_t is the pressure ratio, TFP_{max} and TFP_{exp} are model parameters. Turbine efficiency is modeled as proposed in Watson and Janota (1982).

$$BSR = \frac{\omega_{tc}\, r_t}{\sqrt{2 c_p T_{03} \left(1 - \Pi_t^{\frac{\gamma_t - 1}{\gamma_t}}\right)}} \tag{2.4}$$

$$\eta_t(BSR) = \eta_{t,max} \left[1 - \left(\frac{BSR - BSR_{opt}}{BSR_{opt}}\right)^2\right] \tag{2.5}$$

Where r_t is the turbine radius, c_p the specific heat at constant pressure and γ_t the ratio of specific heats. BSR_{opt} and $\eta_{t,max}$ are model parameters.

Figure 2.2 shows that the mass flow model fits the data well. Not much can be said about the efficiency model on the other hand. The measured points are too close to determine if the behavior of the system is captured sufficiently. The turbine efficiency validation is left as a model to validate by using the full turbocharger model and time resolved step data.

2.1.2 Compressor

The compressor massflow and efficiency are modeled using LiUCPgui (Llamas and Eriksson, 2016, 2017, 2018), which is a *MATLAB* compressor modeling toolbox. The ellipse massflow model used in the toolbox was originally proposed in Leufvén and Eriksson (2013).

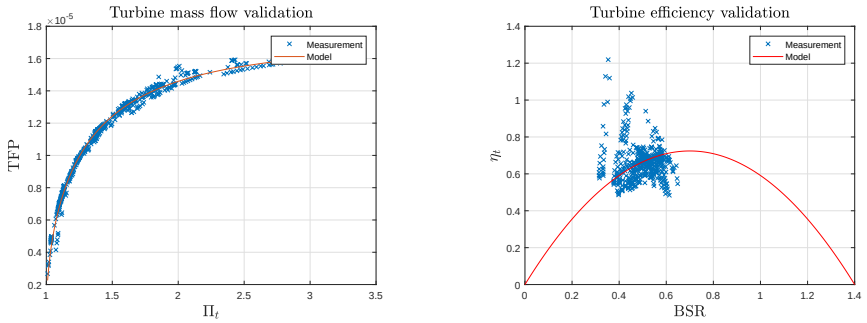

Figure 2.2: *Turbine mass flow and efficiency validation, measured data versus model. The turbine mass flow model shows accurate fit, while nothing can be said for the efficiency model.*

$$\bar{N}_c = \omega_{tc} \frac{1}{\sqrt{T_{01} \,/\, T_{c,ref}}} \tag{2.6}$$

$$\bar{W}_c = \dot{m}_c \frac{\sqrt{T_{01} \,/\, T_{c,ref}}}{p_{01} \,/\, p_{c,ref}} \tag{2.7}$$

$$\bar{N}_{c,n} = \bar{N}_c / \bar{N}_{c,max} \tag{2.8}$$

$$\bar{W}_{Ch}(\bar{N}_{c,n}) = \bar{W}_{c,max} \ldots \\ \ldots (C_{Wch,1} + C_{Wch,2}\ arctan(C_{Wch,3}\bar{N}_{c,n} - C_{Wch,4})) \tag{2.9}$$

$$\Pi_{Ch}(\bar{N}_{c,n}) = \Pi_{c,max}(C_{\Pi ch,1} + C_{\Pi ch,2}\bar{N}_{c,n}^{C_{\Pi ch,3}}) \tag{2.10}$$

$$\bar{W}_{ZS}(\bar{N}_{c,n}) = \bar{W}_{c,max}(C_{Wzs,1}\bar{N}_{c,n}^{C_{Wzs,2}}) \tag{2.11}$$

$$\Pi_{ZS}(\bar{N}_{c,n}) = 1 + (\Pi_{c,max} - 1)C_{\Pi zs,1}\bar{N}_{c,n}^{C_{\Pi zs,2}} \tag{2.12}$$

$$CUR(\bar{N}_{c,n}) = C_{cur,1} + C_{cur,2}\bar{N}_{c,n}^{C_{cur,3}} \tag{2.13}$$

$$\Pi_c = \frac{p_{02}}{p_{01}} \tag{2.14}$$

$$\bar{W}_c = \bar{W}_{ZS} + \ldots \\ \ldots (\bar{W}_{Ch} - \bar{W}_{ZS})\left[1 - \left(\frac{\Pi_c - \Pi_{Ch}}{\Pi_{ZS} - \Pi_{Ch}}\right)^{CUR}\right]^{\frac{1}{CUR}} \tag{2.15}$$

Where $\dot{m}_c$ is the compressor massflow, and $C_{Wch\ldots cur}$ are model parameters. $\bar{N}_{c,max}$, $\bar{W}_{c,max}$ and $\Pi_{c,max}$ are values taken from the map. Π_c is the compression ratio. The enthalpy-based compressor efficiency is modeled as proposed in Llamas and Eriksson (2016, 2017).

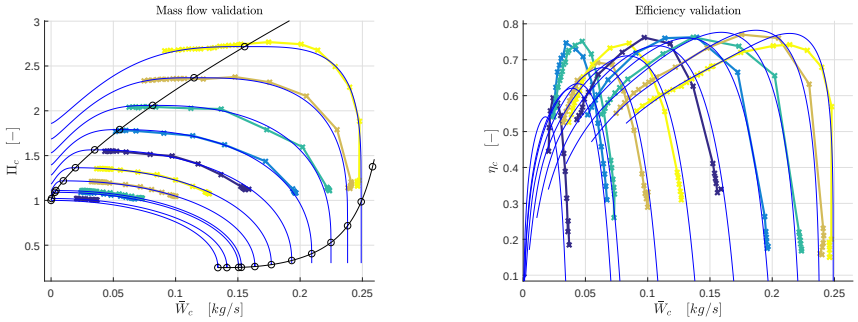

Figure 2.3: *Compressor mass flow and efficiency validation, measured data versus model. The ellipse model shows great fit, while the efficiency data looks irregular and two speed-lines seem out of place.*

$$\eta_c = \frac{\Delta h_{0s}}{\Delta h_{act}} \tag{2.16}$$

$$\Delta h_{0s} = c_p T_{01} \left[\Pi_c^{\frac{\gamma-1}{\gamma}} - 1 \right] \tag{2.17}$$

$$\Delta h_{act} = (1 + k_{loss}(\bar{N}_c, \bar{W}_c))(b(\bar{N}_{c,n}) - a(\bar{N}_{c,n})\bar{W}_c) \tag{2.18}$$

$$b(\bar{N}_{c,n}) = \Delta h_{act,max}(C_{b,1}\bar{N}_{c,n}^2 + C_{b,2}\bar{N}_{c,n}^3) \tag{2.19}$$

$$a(\bar{N}_{c,n}) = \frac{\Delta h_{act,max}}{\bar{W}_{max}} \frac{C_{a,1}\bar{N}_{c,n}}{(1 + C_{a,2}\bar{N}_{c,n}^2)^{C_{a,3}}} \tag{2.20}$$

$$k_{loss}(\bar{N}_c, \bar{W}_c) = \frac{C_{loss}\rho_{01}D_2^3\pi\bar{N}_c}{60\bar{W}_c} \tag{2.21}$$

Where C and C_{loss} are model parameters. $\Delta h_{act,max}$ is the maximum work value of the map, D_2 the compressor impeller diameter, and ρ_{01} the inlet density. T_{01} is the ambient temperature and η_c the compressor efficiency. The charge pressure is modeled as a massflow balance.

$$\dot{p}_{02} = \frac{R_{air}T_{02}}{V}(\dot{m}_{in} - \dot{m}_{out}) \tag{2.22}$$

Where V is the volume of the pipe from the compressor to the valve.

Figure 2.3 shows that the compressor mass flow fits well with the data. The zero slope and choke line, is consistent when compared to other cases where a model was parameterized for the Mitsubishi TD04 turbocharger, such as Llamas and Eriksson (2017). This implies that the mass flow model is valid.

The compressor efficiency model fits relatively well to the data. There are two

speed-lines, for low mass flows, which are outliers. The two anomalous speed-lines should probably have been removed for a better model fit.

2.1.3 Shaft

The friction is modeled using Petroff's law of friction torque in bearings. The turbocharger speed is modeled with Newton's second law, using a balance of torques on the shaft.

$$T_{q,f} = (c_{f,0} + c_{f,1}\omega_{tc})\mu_{oil} \tag{2.23}$$

$$\dot{\omega}_{tc} = \frac{1}{J_{tc}}(T_{q,t} - T_{q,c} - T_{q,f}) \tag{2.24}$$

Where $T_{q,t}, T_{q,c}, T_{q,f}$ are the turbine, compressor and friction torque, J_{tc} is the rotational inertia (wheels and shaft) and μ_{oil} is the oil viscosity. $c_{f,0}$ and $c_{f,1}$ are model parameters.

2.1.4 Butterfly valve

The valve is modeled as proposed in Eriksson and Nielsen (2014).

$$\Pi\left(\frac{p_{aft,bv}}{p_{bef,bv}}\right) = max\left(\frac{p_{aft,bv}}{p_{bef,bv}}, \left(\frac{2}{\gamma_c + 1}\right)^{\frac{\gamma_c}{\gamma_c - 1}}\right) \tag{2.25}$$

$$\Psi_0(\Pi) = \sqrt{\frac{2\gamma_c}{\gamma_c - 1}(\Pi^{\frac{2}{\gamma_c}} - \Pi^{\frac{\gamma_c+1}{\gamma_c}})} \tag{2.26}$$

$$\Psi_{li} = \begin{cases} \Psi_0(\Pi), & if\ \Pi_{bv} \leq \Pi_{li} \\ \Psi(\Pi_{li})\frac{1-\Pi}{1-\Pi_{li}}, & otherwise \end{cases}$$

$$\dot{m}_{bv} = \frac{p_{bef,bv}}{\sqrt{RT_{bef,bv}}} A_{bv}(\alpha) c_{d,bv}(\alpha) \Psi_{li}\left(\frac{p_{aft,bv}}{p_{bef,cv}}\right) \tag{2.27}$$

$$A_{bv}\ c_{d,bv} = c_{b,0} + c_{b,1}\alpha + c_2\alpha^2 + c_3\alpha^3 \tag{2.28}$$

Where $\frac{p_{aft,bv}}{p_{bef,bv}}$ is the pressure ratio over the valve, A_{bv} is the effective area of the restriction, $c_{b,0\ldots3}$ are model parameters, and where the linear region is defined by $\frac{p_{aft,bv}}{p_{bef,bv}} \epsilon\ [\Pi_{li}, 1]$.

Figure 2.4 shows that the friction model fit is uncertain. The measured data points shows somewhat linear behavior, but not much can be said without the full turbocharger model validation. The buttefly valve however shows great fit to the measured data. The measured data only goes as low as $\alpha \approx 0.2$, which means that extrapolating the model to lower valve angles can introduce errors. A lower limit on α is therefore set for the optimal control, which will be described in later sections.

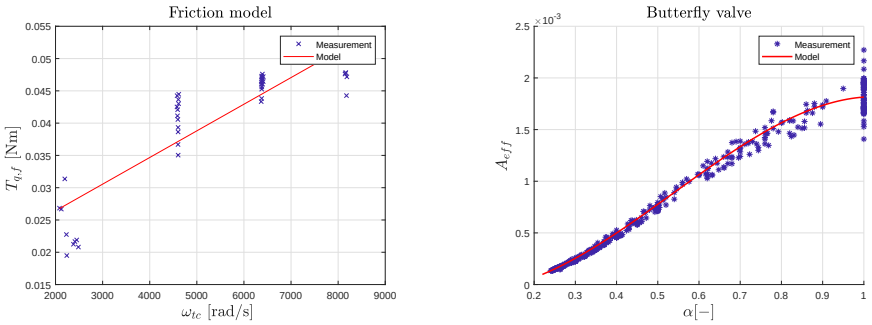

Figure 2.4: *Friction (left) and butterfly valve (right) validation, measured data versus model. The friction data seems to have a fairly linear behavior, but more data points are need to accurately judge the model fit. The butterfly valve model shows good fit.*

2.2 Heat Transfer

Heat transfer occurs in three ways, conduction, convection and radiation. Conduction is the internal heat transfer in a solid object, convection is the heat transfer occuring between a gas and a solid, and radiation is the objects emission of electromagnetic waves.

The heat transfer system, shown in Figure 2.5, is modeled as a lumped capacity system with three thermal masses, proposed in Baines et al. (2010). The convection is modeled as:

$$\dot{Q}_{conv} = c(\dot{V}_t/\nu)^{c_1} \lambda Pr^{c_2}(T_{gas} - T_i) \tag{2.29}$$

Where $\dot{V}_t$ is the fluid volume flow, ν is the kinematic viscosity, λ is the thermal conductivity, Pr is the Prandtl's number. c and $c_{1,2}$ are model parameters. T_i is the component temperature, which is either T_t, T_{bh} or T_c.

The conduction between two components is modeled as:

$$\dot{Q}_{cond} = c(T_i - T_j) \tag{2.30}$$

Where T_i and T_j are the component temperatures, and c is a model parameter.

The combined convection and radiation of a component to the atmosphere is modeled as:

$$\dot{Q}_{ext} = c(T_i - T_{atm}) \tag{2.31}$$

The cooling effect of the water and oil systems are represented using the model for convection.

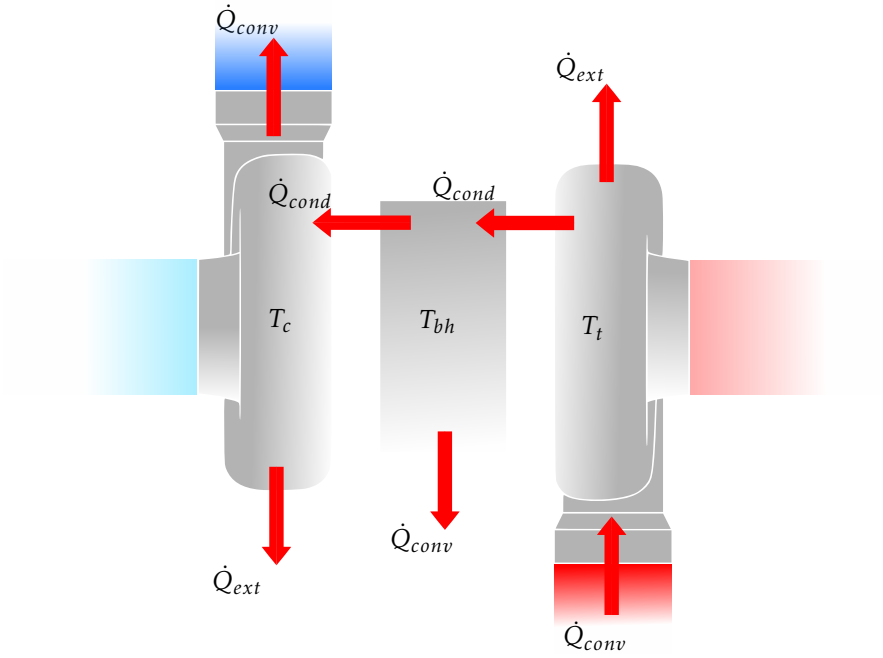

Figure 2.5: *Overview of the heat transfer system. Three convections, two conductions and two external heat transfers. Three temperature states, one for each component.*

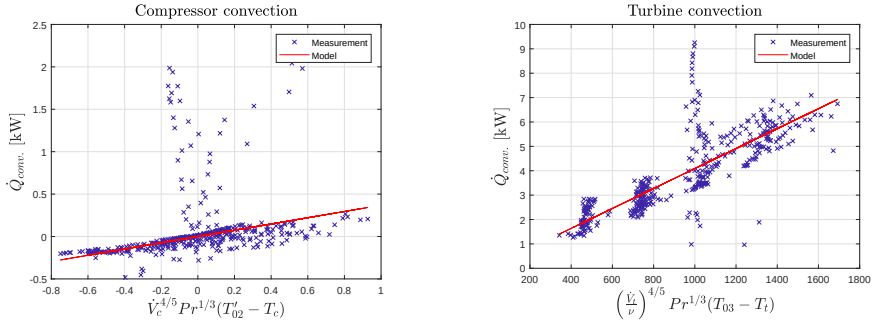

Figure 2.6: *Convection model validation, measured data versus model. The compressor convection model fits the data well, except for the cloud of outliers seen in the middle of the figure. The same holds for the turbine convection.*

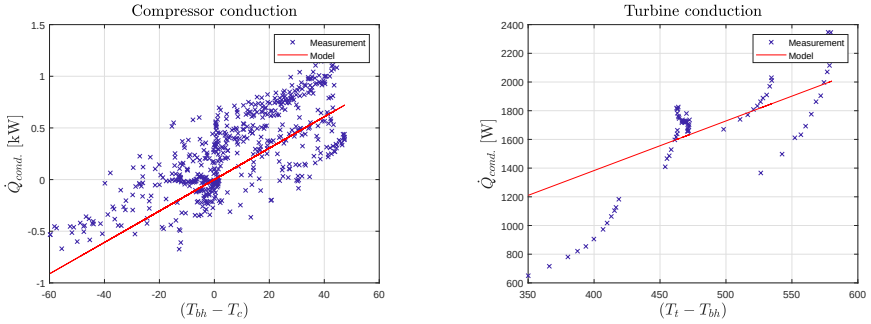

Figure 2.7: *Conduction model validation, measured data versus model. The compressor conduction data shows linear behavior, but a high variance. The turbine conduction model fit is hard to judge.*

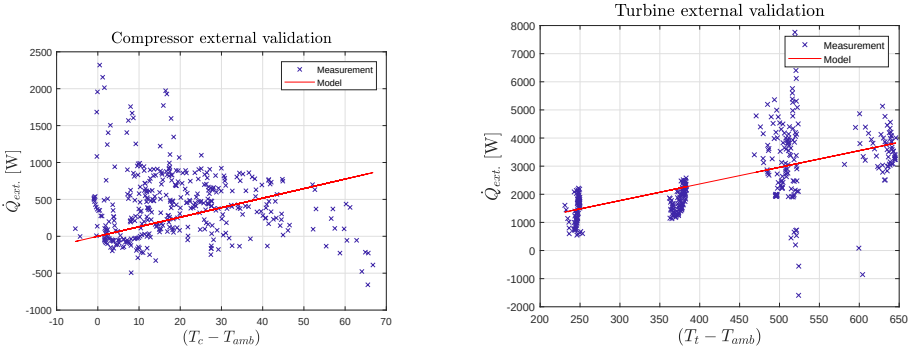

Figure 2.8: *External heat transfer model validation, measured data versus model. The compressor external heat transfer model does not show good fit. The turbine model fits relatively well, however.*

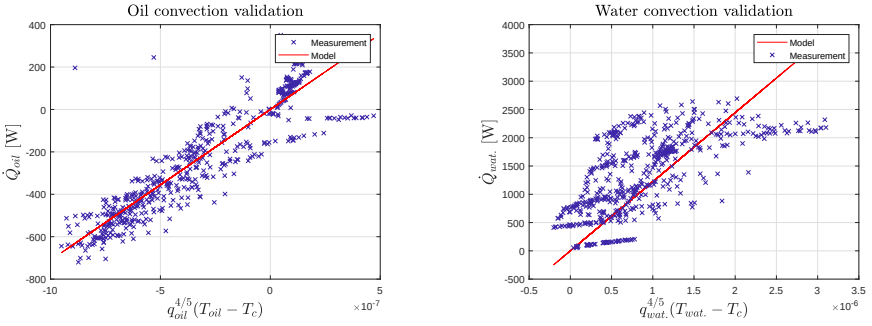

Figure 2.9: *Cooling convection model validation, measured data versus model. Both the oil and water convection model show good fit to the data.*

Each temperature T_t, T_{bh} and T_c are modeled by a heat transfer balance:

$$\dot{T}_i = \frac{1}{c_{p,i} m_i} \left(\sum \dot{Q}_{in} - \sum \dot{Q}_{out} \right) \tag{2.32}$$

Where m_i is the component mass, $c_{p,i}$ is the component specific heat.

Figure 2.6 shows that the convection models fit the data well. The compressor convection data has a few outliers around the zero, but these are ignored for a better linear fit. The same kind of outliers show in the turbine convection, around the 1000 mark.

In Figure 2.7 the turbine and compressor conduction fits are presented. The compressor conduction shows a linear behavior, but seemingly high variance. The turbine conduction lacks the data necessary to judge fit.

The compressor external heat transfer validation is inconclusive. The data points are far to scattered to0 judge the model fit as accurate. The turbine external heat transfer validation shows signs of linear behavior however, with a few outliers between the 500-600 mark. The cooling model fits in Figure 2.9 show quite accurate fit for the oil, but less so for the water.

2.3 Full Model Validation

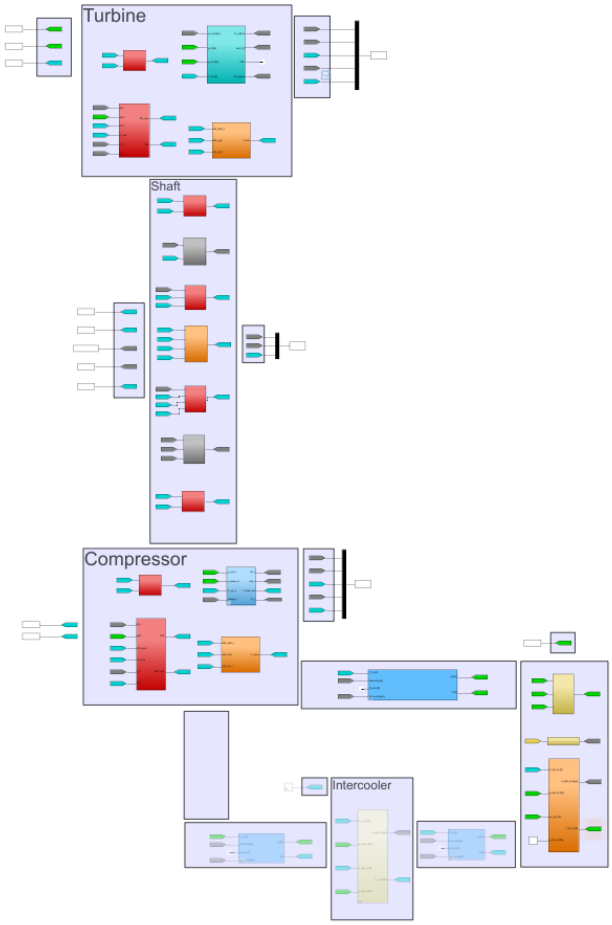

Figure 2.10: *Simulink model of the complete turbocharger and the needed gas stand components. The model is split, visually, in three parts, turbine, shaft, and compressor. The intercooler and its connecting control volumes have been commented out, since only the closed loop case is considered.*

To validate the complete model, a sequence of step responses are simulated using a simulink model presented in Figure 2.10, and compared to measured data. The results are presented in Figure 2.11, 2.12, and 2.13. The dynamics in the system are captured quite well, which is important for the optimal control. The steps were made by increasing the exhaust pressure p_{03}. In the simulink model, the valve angle α is controlled by a PI controller to match the measured pressure ratio over the compressor. The exhaust temperature T_{03} is kept constant at 873 Kelvin.

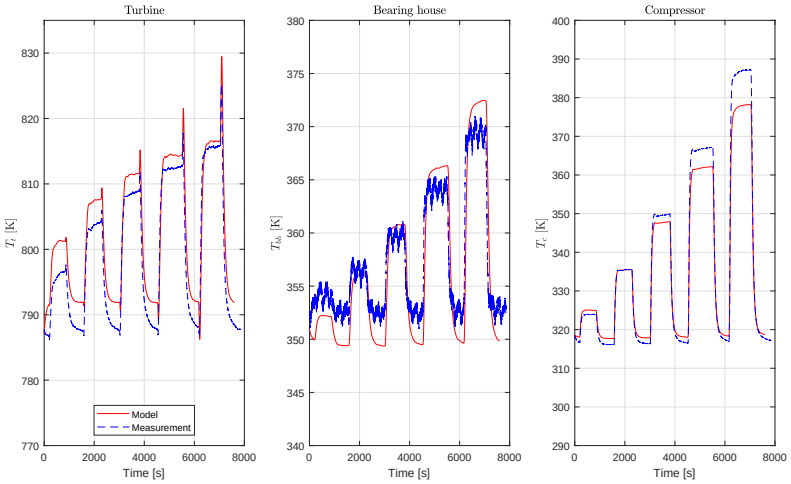

Figure 2.11: *Turbine, compressor, and bearing house temperature, measured data versus model. The model fit for the three temperatures is decent, with a maximum error of roughly 5 Kelvin. The turbine model fits high temperatures best, the bearing house the middle, and the compressor for low temperatures.*

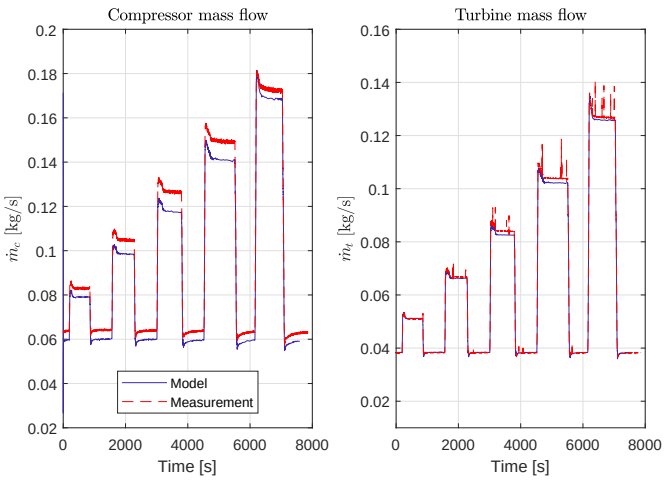

Figure 2.12: *Compressor and turbine massflow, measured data versus model. The turbine mass flow model fits the data very well. The compressor mass flow model fits decently, but a small stationary error is seen, with a maximum error of roughly 0.01 kg/s.*

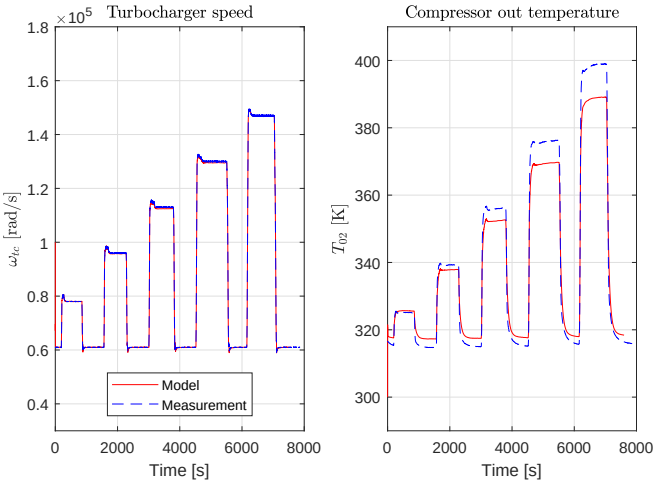

Figure 2.13: *Turbocharger speed and compressor outlet temperature, measured data versus model. The turbocharger speed has a very low error, which indicates that the turbine and compressor efficiencies, as well as the friction models are valid. The compressor out temperature fits decently, with a maximum error of roughly 10 Kelvin.*

3

Optimal Control

3.1 Short Introduction

The typical optimal control setup can be described by posing an optimization problem, where the cost function is an integral, and the constraint is a differential equation. A term to penalize the final state is also added.

$$\begin{aligned} \min_{u} \quad & \Phi(x_f) + \int_{t_i}^{t_f} f_0 \, dt \\ \text{subject to} \quad & \dot{x}(t) = f(t, x(t), u(t)) \\ & x(t_i) = x_0, \; u \, \epsilon \, U \end{aligned}$$

The goal is to find a trajectory $u^*(x, t)$ (a starred variable signifies optimality) that minimizes the cost function, which could be quadratic $f_0 = x^T Q x + u^T R u$. A common cost function that minimizes the time $t_f - t_i$ is $f_0 = 1$. There exists many tools to solve the optimal control problem analytically. For example, the Hamilton-Jacobi-Bellman equation (HJBE):

$$\frac{\delta V}{\delta t} = \min_{u} \left\{ f_0 + \frac{\delta V}{\delta x} \, f \right\}$$

The HJBE, a partial differential equation, is difficult to solve. For some problems where f_0 is quadratic and no input or state constraints exist, the HJBE simplifies to the Riccati equation. Solving the HJBE provides closed loop control, but there is an easier method that provides open loop control which is called

Pontryagins minimization principle (PMP). Although simpler than HJBE, PMP is also impractical for complex systems with a moderate to high amount of states. The most common method today is to use numerical optimal control.

The *direct* methods of numerical optimal control consists of first discretizing a problem, then optimization by a non-linear program (NLP):

$$\begin{aligned} \min_{w} \quad & f(w) \\ \text{subject to} \quad & lb_g \leq g(w) \leq ub_g \\ & lb_w \leq \ w \ \leq ub_w \end{aligned}$$

Where f is the cost function, w the decision variables, and g the constraint equations. The method of discretization used in this thesis project is *direct collocation*, where the differential equation is approximated by a polynomial, in a specified number of *collocation points*.

3.2 Optimal Control Problem Setup

The goal is to reach steady state as fast as possible, with specified final values for ω_{tc}, p_{02}, and T_{03}. The upper and lower bounds are summarized in Table 3.1, along with the maximum input signal rate of change. $\dot{u}_{max}$ is chosen so that the optimal control signals are achievable in a real gas stand.

Table 3.1: *Upper and lower bounds on states, inputs and input rate of change.*

Var.	lb	ub	$\dot{u}_{max}$
ω_{tc} [rad/s]	5000	18000	-
p_{03} [bar]	1	4.5	0.1
p_{02} [bar]	1	-	-
T_{03} [K]	300	1200	100
T_t [K]	300	1000	-
T_{bh} [K]	300	400	-
T_c [K]	300	400	-
α [-]	0.05	1	0.1
T_{oil} [K]	330	373	10

The upper and lower bounds of the states and inputs, are abbreviated as lb_x/ub_x, lb_u/ub_u, and $\dot{u}_{max}$. The optimal control problem (OCP) can then be written as:

$$\min_{u} \quad \int_{t_i}^{t_f} 1 \; dt \tag{3.1}$$

$$\text{subject to} \quad \dot{x}(t) = f(t, x, u) \tag{3.2}$$

$$lb_x \leq x \leq ub_x \tag{3.3}$$

$$lb_u \leq u \leq ub_u \tag{3.4}$$

$$|\dot{u}| \leq \dot{u}_{max} \tag{3.5}$$

$$x(t_i) = x_0 \tag{3.6}$$

$$x_{4,5}(t_f) = x_{ref,t_f} \tag{3.7}$$

$$\dot{x}(t_f) = 0 \tag{3.8}$$

Where f is the turbocharger and heat transfer model and $[t_i, t_f]$ denotes the start and end time. Equation 3.2-3.8 defines the OCP constraints. The OCP is discretized with direct collocation, using the Legendre points. The collocation method is implemented with CasADi (Andersson, 2013), and the resulting nonlinear program is solved using IPOPT (Wächter, 2013).

Additional constraints are added to the OCP. One is that the turbocharger must stay in the area defined by the compressor surge and choke lines (the surge and choke lines are the upper and lower bounds for the working region in the compressor map).

3.3 NLP Transcription

CasADi is mainly an automatic/algorithmic differentiation software, but it has an easy to use interface to many state of the art optimization solvers.

Assume piecewise constant control u_0 ... u_N, over N intervals, which are equidistant in time. On each interval, the state trajectory is interpolated by a Lagrange polynomial, in a number of collocation points d. A very useful property of Lagrange polynomials, is that the coefficients x_j assume the same value as $x(t)$ in the collocation points.

$$L(t) := \sum_{j=0}^{d} x_j \; l_j(t), \quad l_j(t) := \prod_{r=0,\; r\neq j}^{d} \frac{t - t_r}{t_j - t_r}$$

The lagrange polynomial is differentiated:

$$L'(t) := \sum_{j=0}^{d} x_j \; l'_j(t), \quad l'_j(t) := \sum_{i=0, i\neq j}^{d} \left[\left(\frac{1}{t_j - t_r} \right) \prod_{r=0,\; r\neq i,j}^{d} \frac{t - t_r}{t_j - t_r} \right]$$

The resulting expression is equaled to the state dynamics, evaluated in each point, to form the *collocation equations*. So for example, the first control interval would produce four equations.

$$L'(0) - f(x_{j,0},\ u_1) = 0, \quad L'(d_1) - f(x_{j,1},\ u_1) = 0$$

$$L'(d_2) - f(x_{j,2},\ u_1) = 0, \quad L'(d_3) - f(x_{j,3},\ u_1) = 0$$

To ensure continuity, the *continuity equations* are posed by forcing the Lagrange polynomial, evaluated at the final time of one interval, to be equal to the inital state value in the next interval.

$$\sum_{n=0}^{N} L_n(1) - x_{0,n+1} = 0$$

Then, the NLP is formed by combining the collocation and continuity equations in $g(w)$, where w, the optimization variables, are the piecewise constant inputs u, and the state vector x, along with the Lagrange coefficients $x_{j,n}$.

$$\begin{aligned} \min_{w} \quad & J(w) \\ \text{s.t.} \quad & g(w) = 0 \\ & lb_w \leq w \leq ub_w \end{aligned}$$

The cost function J is formed by a quadrature.

$$J(w) \approx \sum_{k=1}^{N-1} \Delta t \sum_{r=0}^{d} \int_0^1 L_r(\tau)\, d\tau\ f_0(\cdot)$$

The NLP is then passed to an external solver. The solver used is IPOPT.

3.4 Results

Three optimal transient example trajectories are presented, shown in Figure 3.1.

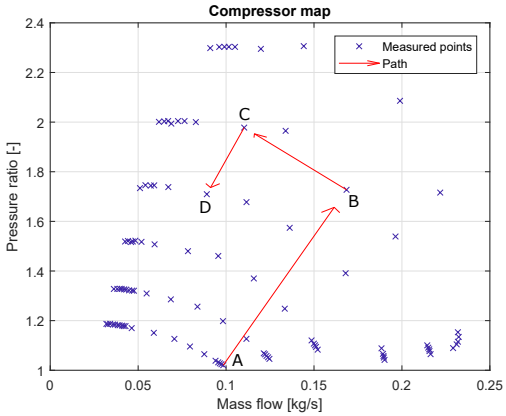

Figure 3.1: *The three presented transient trajectories, shown point to point. Three OCP's are solved, to make time optimal transitions between A-B, B-C and C-D. The end-criterions are thermal equilibrium, and Π_c and ω_{tc} reaching the value specified in the compressor map.*

Figure 3.2 shows the optimal path from point A to point B. It is not surprising that going from a low to high energy point leads to an increase in material temperature. Therefore, reaching steady state quickly, is a matter of pumping heat into the bearing house. According to the solution in Figure 3.2, the maximum heat transfer (from the air to the compressor) occurs for high rotational speed and low charge pressures. T_{03} also increases during the transient to increase the flow of heat through the bearing house.

When the compressor convection is examined, as in Figure 3.3, it can be seen that a high speed and low pressure does maximize the heat transfer, which indicates that the generated optimal trajectories are valid. A suitable comparison for the optimal control method, would be to apply the inputs that would produce the correct steady state values, and simply wait until the system reach thermal equilibrium. The correct input values are already known from the optimization, $u(t_f)$.

Figure 3.4 shows that the constant input method reaches steady state at approximately 240 seconds. The optimal control method reaches steady state at 19 seconds, a reduction of time by a factor of 12.5.

Figure 3.5 shows the optimal path from point B to point C. It shows similar trajectories from the previous path. An interesting behavior is that the temperatures in the bearing house and compressor have the same characteristics, indicat-

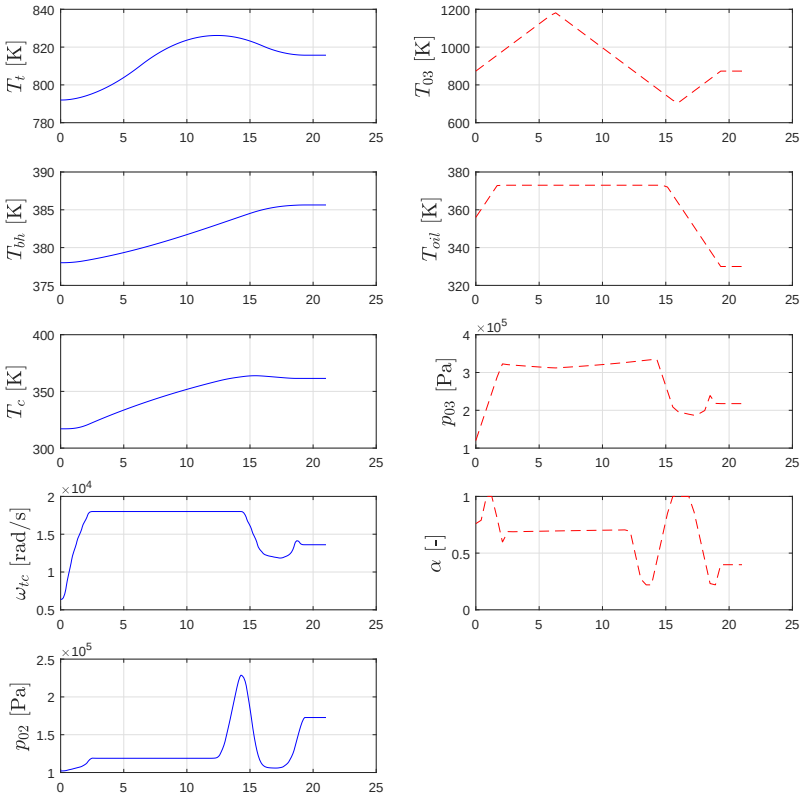

Figure 3.2: *First example of optimal trajectories. The figure shows the trajectories from point A to point B. Increasing the temperature of all components requires high speeds, low pressures and high exhaust gas temperatures.*

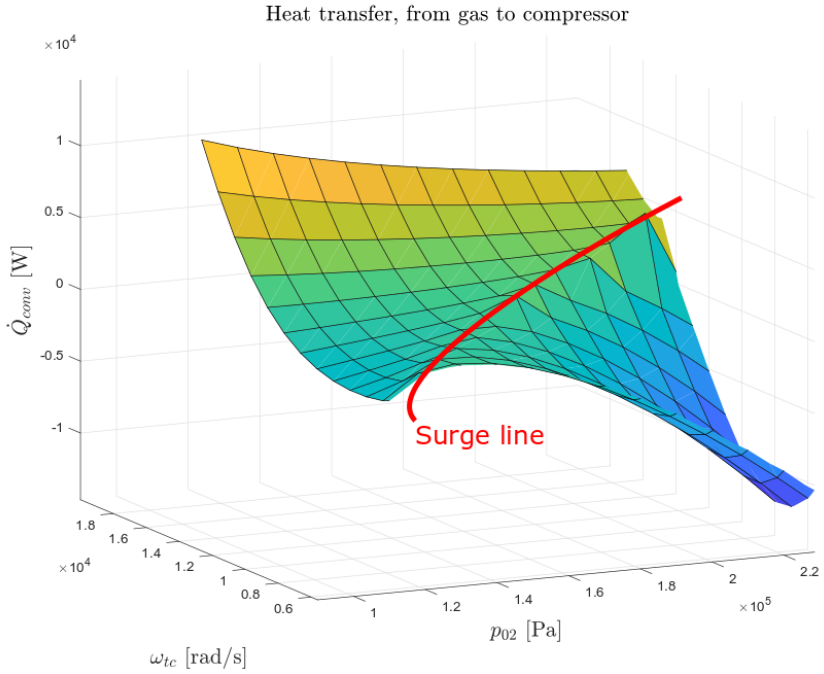

Figure 3.3: *Compressor convection as a function of ω_{tc} and p_{02}, and the mean T_c. High speeds and low pressures result in the maximum amount of heat transfer to the compressor.*

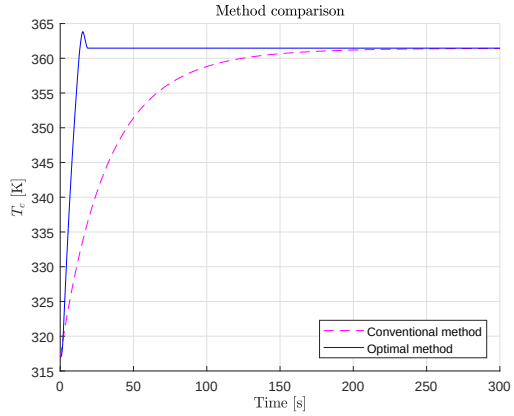

Figure 3.4: *Optimal control method versus constant input. The conventional method, meaning letting the system reach steady state using constant inputs, is much slower.*

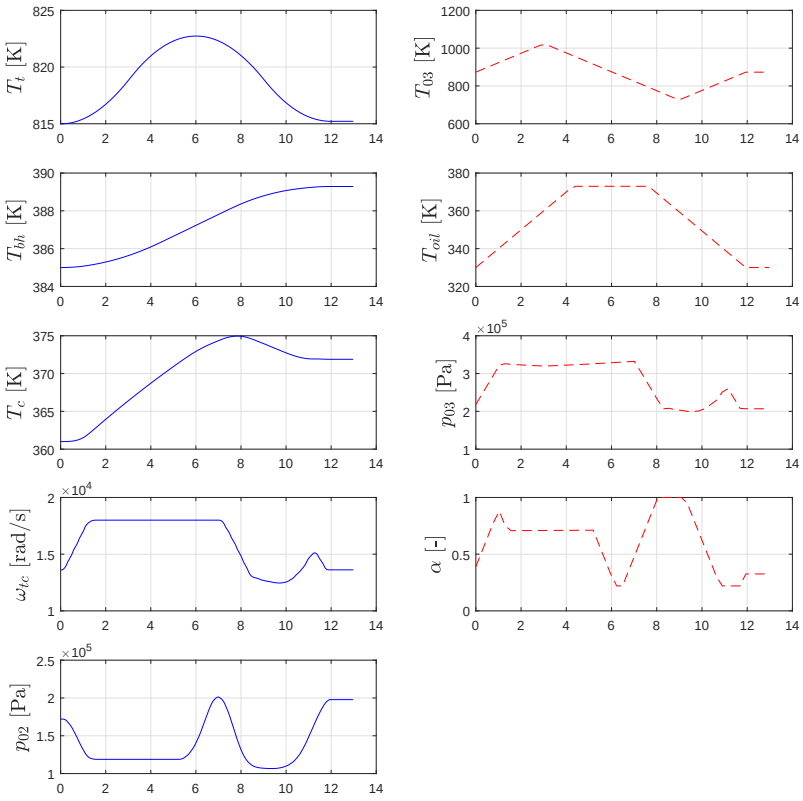

Figure 3.5: *Second example of optimal trajectories. The figure shows the trajectories from point B to point C. Increasing the temperature of all components requires high turbocharger rotational speeds, low pressures and high exhaust gas temperatures.*

ing that the bottleneck is the bearing house temperature. This is true because the compressor temperature in both cases, rises above its final value to aid the bearing house in heating. Replicating the methods from transient A-B, the optimal control method for this case shows a reduction of time by a factor of 21.

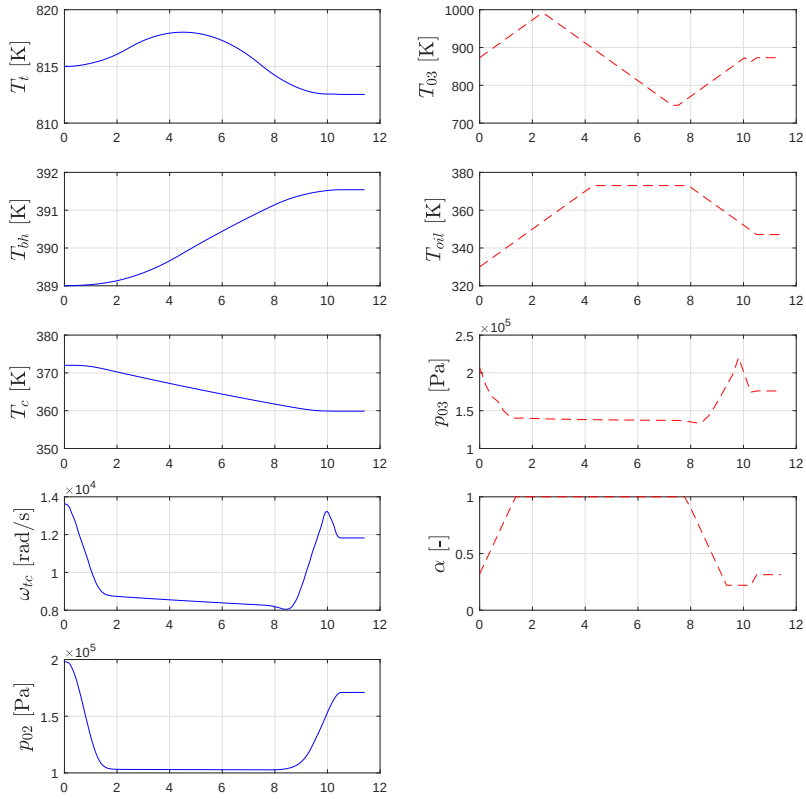

Figure 3.6: *Third example of optimal trajectories. The figure shows the trajectories from point C to point D. For this case, the bearing house heats up while the turbine and compressor cools down. Cooling the compressor requires low speeds and low pressures. The turbine heats up at first, in order to heat up the bearing house.*

Figure 3.6 shows the optimal path from point C to point D. For this path, the optimization code finds trajectories where the bearing house temperature increases, but the compressor cools down. Consistent with the results in Figure 3.3, cooling the compressor optimally should require slow speeds and low pressures.

Time reduction for this case is a factor of 23.

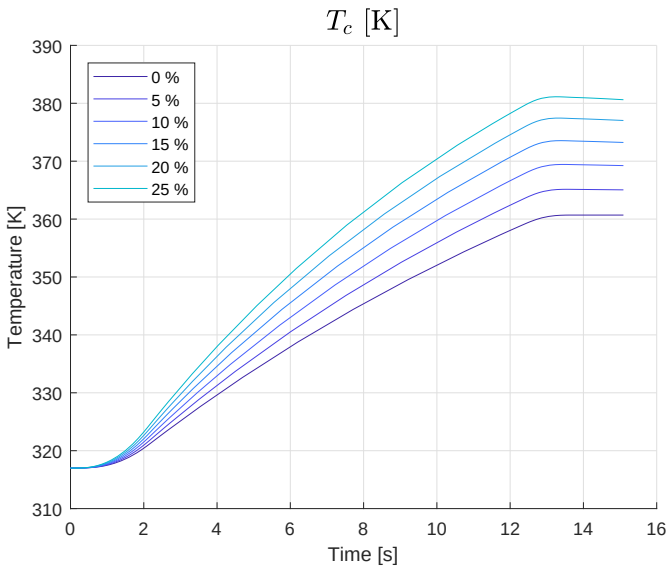

Figure 3.7: *Result of scaling the model parameters by a certain percentage. The parameter errors result in a large offset at the end, but still very close to steady state.*

The optimal control is calculated using a known map. This poses problems when measuring on a new turbocharger, when the compressor load points might not be known in advance. In Figure 3.7, the results of using the input signals from Figure 3.2, on a turbocharger model with scaled parameters, are presented. All model parameters are increased by the percentage value shown in Figure 3.7. The steady state values of the temperatures are quite sensitive to parameter error. The system almost reaches steady state at the same time, however.

3.5 Optimal Sequence of Transients

The original compressor map consists of 100 points. A new map is created where some points have been merged. The amount of points is reduced to 43, to be more computationally manageable. Very close points in the map are therefore merged. Figure 3.8 shows the new compressor map.

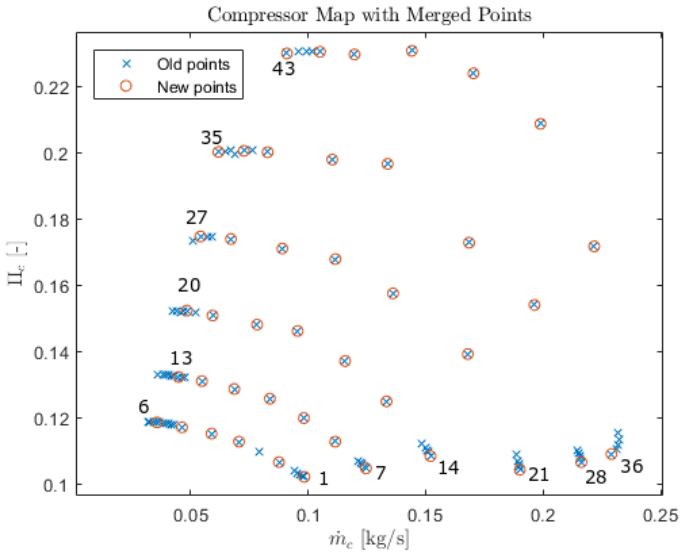

Figure 3.8: *Merged operating points of the compressor map. The new merged map contains 43 points. The points are numbered by speedline as the figure shows.*

An optimal route through the target operating points have been found using results in the previous section. Since it is now possible to traverse the set of operating points optimally, a cost matrix can be calculated. It is done simply by calculating the time it takes to go from all points to every other point. Finding the fastest route through a compressor map is an open travelling salesman problem and the cost matrix is presented in Figure 3.9.

In general, traversing a path from a high power point, to a low power point takes longer time than in reverse. The worst case is over two minutes (seen to the right in Figure 3.9). This behavior can be explained by the disproportionate amount of heating power relative to cooling. The burner can produce a lot of heat and transfer it to the turbine, while the cooling potential is much lower.

In contrast, traversing from a point with low power to a point with higher power is faster, as described by the red and green zone in Figure 3.9.

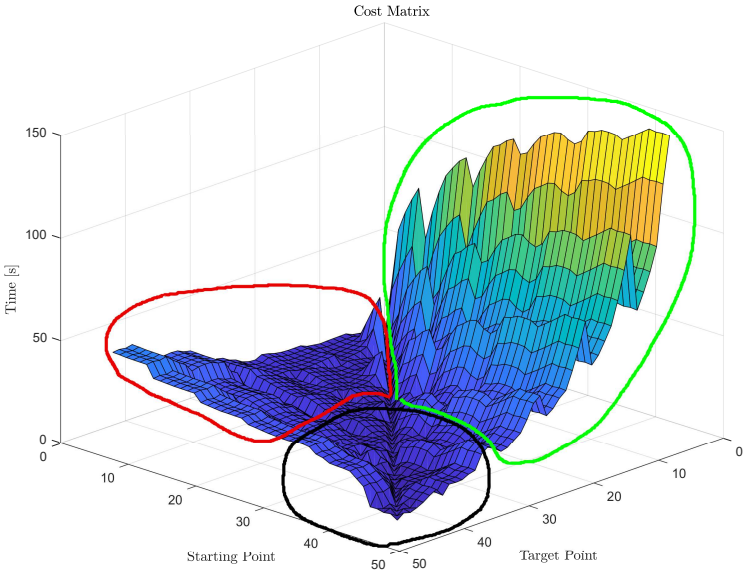

Figure 3.9: *The travelling salesman cost matrix. The figure shows the time cost of traversing the compressor map, with optimal trajectories. The matrix can be roughly divided into three sections, red, green and black. In the red and green area, heating is faster than cooling, but in the black, the heating and cooling potential is roughly equal. Costs in the green zone are associated with cooling, while costs in the red zone are associated with heating.*

However, that is only accurate for the red and green zones. In the black area, the cooling and heating potential is roughly equal. When the material temperatures of the turbocharger are higher, the cooling power increases.

A fast and near optimal method to find the best route through the compressor map, is to use a genetic algorithm. A genetic algorithm starts by randomizing a population, in this case of 200 routes. The best routes of the population are chosen, and are mutated slightly to form the next iteration of 200 specimens (routes). The near optimal solution is then found by repeating this process. The code used is from Kirk (2014). The result of finding the near optimal path is shown in Figure 3.10.

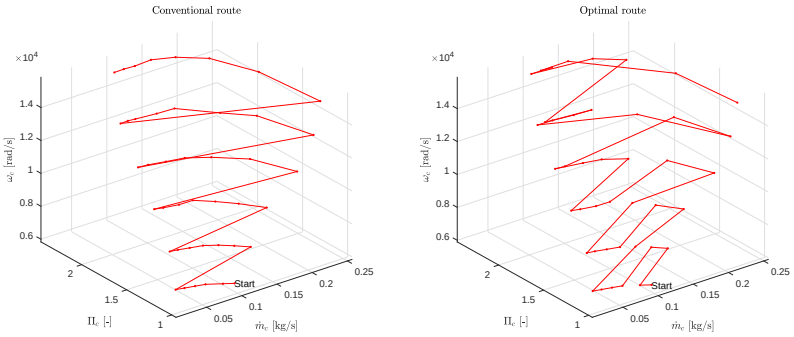

Figure 3.10: *The measured and near optimal route through the set of operating points.*

The same method as in the previous section, is used to compare the results. The comparison is best to worst case scenario, meaning using an optimal route and optimal control, versus a suboptimal route with the constant input (constant burner temperature) point to point method. For the worst case, the simulations are terminated when the system is very close to steady state. This method produces a test time of approximately 3.5 hours.

The total time for the best case method, can be calculated by adding the elements of the cost matrix that correspond to the optimal route. The total time is then 3 minutes, a time reduction by a factor of 74. However, most of this is due to the point to point optimal trajectory. If the suboptimal sequence of transients is used, but with optimal point to point trajectories, a factor of 63 is seen. The gain of finding the optimal sequence of transients is no more than 30 seconds.

Figure 3.11 shows an effort to explain the optimal path. The red lines shows the simulated system, using constant input to reach steady state, but with the optimal route (to the right in Figure 3.10). The optimal route is to increase the temperatures slowly, and more linear than the conventional route, until a certain

point, where taking a higher step is taken, and then cooling is more time efficient. The higher step occurs when the operating points left to measure is the black zone of Figure 3.9.

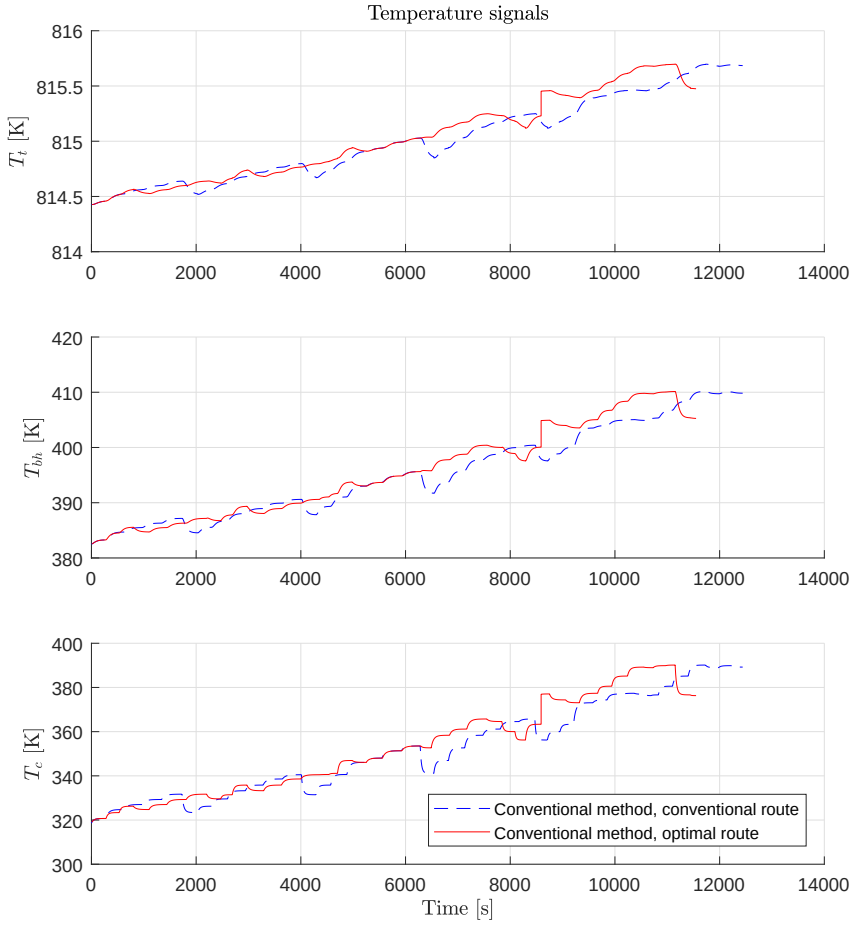

Figure 3.11: *Turbine, compressor and bearing house temperature when using constant inputs to find the steady state temperature value. The two different routes are compared.*

The results mean that, if one would include a 5 minute warm-up period of the burner and gas stand and add 20 seconds for performing each stationary measurement, a compressor map of 43 points would take 22 minutes.

4

System Identification

4.1 The Parameter Estimation Problem

A turbocharger model is needed to use the optimal control method developed in earlier sections. The model is parameterized by using data from turbocharger measurements, a catch-22 situation, since the method is developed to make time efficient measurements. To avoid it, system identification is used to find sufficiently accurate model parameters, using data gathered in a warm-up period before the actual measurements begin.

The full set of parameters is not necessary to estimate. The optimization returns signals for turbine and compressor mass flow, and turbocharger rotational speed, which can be tracked by simple PID controllers. The parameters associated with the mass flow models are therefore not needed. The turbine efficiency model can be neglected aswell, since the untouched T_{03} is easily measured. However, the compressor efficiency model is necessary to identify, since T'_{02} (the charge air temperature before any heat transfer has occured with the compressor material) is practically impossible to measure. The parameters needed to be estimated are associated with the friction, heat transfer, and compressor efficiency models.

The parameter estimation problem is a special case of the general OCP. The necessary parameters can be estimated using the data from a 10 minute warm-up phase, before the actual turbocharger measurements. The method used in this thesis does not require any prior knowledge of the turbocharger, except the order of magnitude of each parameter.

The data used for the parameter estimation, is a simulation of the warm-up

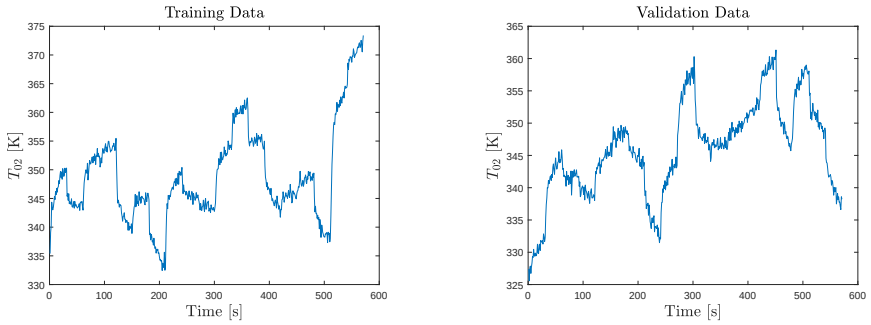

Figure 4.1: *Example signal of the two datasets. One to use when estimating the parameters, and the other to validate them.*

phase of the turbocharger. For 10 minutes (or 600 seconds) the gas stand is simulated, and data is sampled at frequency $f_s = 1\ Hz$. The inputs are white noise filtered through a first order system, so that they form physically achievable signals. Two datasets are produced, for separate training and validation. An example signal of the two sets is shown in Figure 4.1.

The parameter estimation problem can be described as

$$\begin{aligned} \min_{\theta} \quad & \int_{t_i}^{t_f} \sum_{k=1}^{4} \sqrt{\left(\frac{z_k - \hat{z}_k}{z_k}\right)^2}\, dt \\ \text{s.t.} \quad & \dot{x}(t) = f_{heat}(t, x, u, \theta) \\ & z = [x(t)\ T_{02}(t)]^T \end{aligned}$$

Where f_{heat} is the heat transfer system, and T_{02} is calculated with the algebraic equation

$$T_{02} = T_{01} - \frac{\dot{Q} - P_c}{c_p\ \dot{m}_c}$$

4.2 Results

The parameter vector θ includes 15 parameters to estimate. The parameters are used in equations 2.16-2.21(compressor efficiency), 2.23 (friction), and 2.29-2.31(heat transfer). The needed measurement signals are turbine mass flow $\dot{m}_t$, compressor mass flow $\dot{m}_c$, charge air pressure p_{02}, turbocharger rotational speed ω_{tc}, the three temperature states T_t, T_{bh}, and T_c and the charge air temperature

T_{02}.

The optimization problem is discretized with CasADi as explained in previous sections, and solved with IPOPT. The relative error between the estimated and true parameter, used to the generate the data, is shown in Figure 4.2.

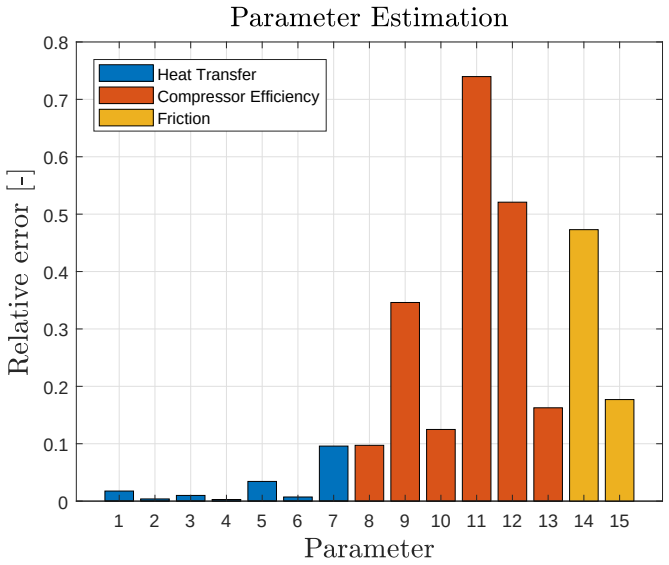

Figure 4.2: *The new estimated model parameters are compared with the model parameters calculated in chapter 2. The estimation method does not find the original true parameters.*

It is clear from Figure 4.2 that the optimization has not found the original set of parameters. However, the set of parameters found, does accurately model the turbocharger as seen, when compared to the validation data, in Figure 4.3. The results show that the optimal control method can be applied to a turbocharger without any prior knowledge of its parameters.

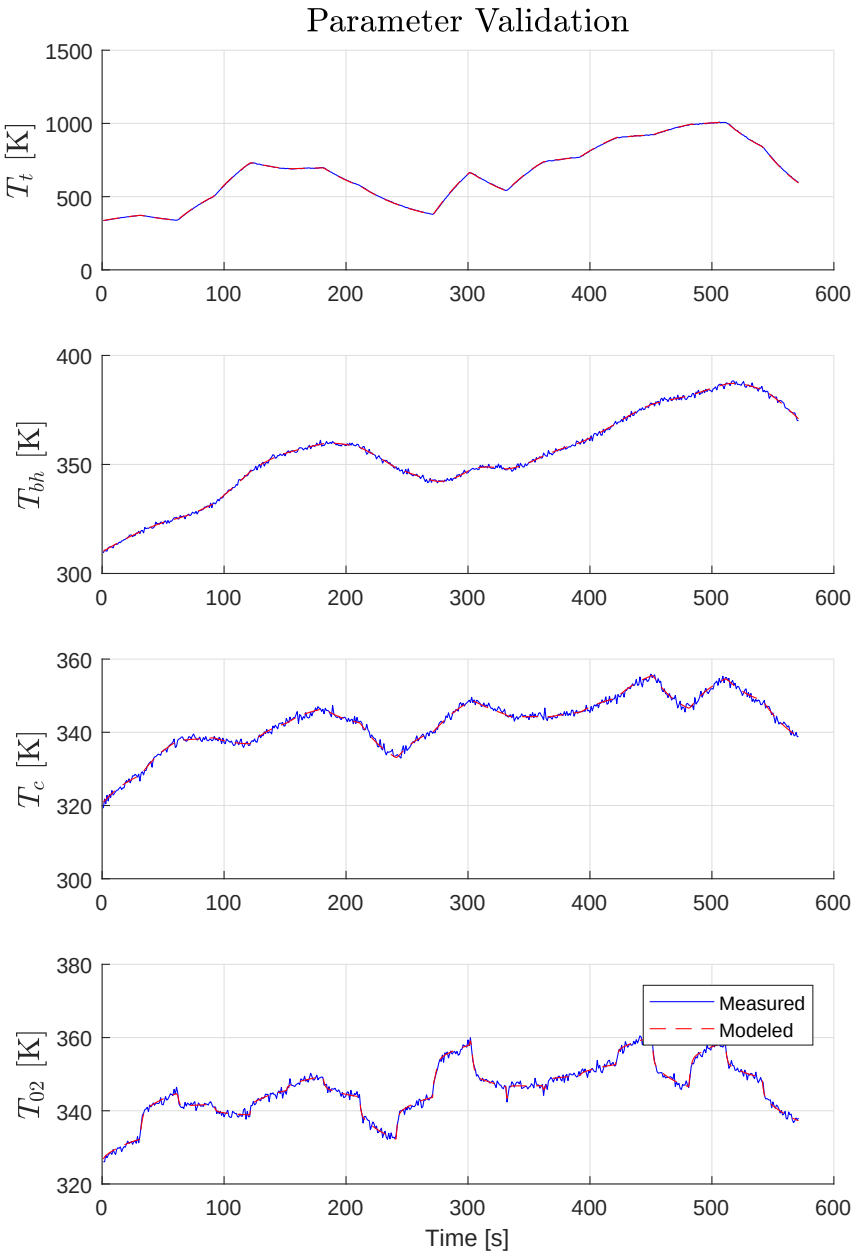

Figure 4.3: *A simulation using the new parameters is compared to the data generated by the old. The estimated parameters can accurately describe the system.*

5

Conclusion and Future Work

5.1 Conclusion

A method for time optimal turbocharger testing has been developed that requires no, or very little, prior knowledge of the turbocharger in question. The method drastically reduces the time required for creating turbocharger maps. By using system identification methods, the problem of model availability and error has been eliminated. The method will be tested experimentally in a gas stand.

A benefit of using the system identification method, even if the optimal control method is not used, is to add corrections to the efficiency map. Since the heat transfer can be calculated for each point in the map, it is possible to then calculate the adiabatic efficiency.

The key conclusions are:

- The turbocharger temperature dynamics is captured by the three state temperature model.
- Optimal control can be applied, using the nonlinear five state model, to solve for the minimum time of the thermal transients that occur between testing points.
- The proposed method can be used to reduce the total testing time significantly.
- Optimal control combined with a traveling salesman problems can be used to determine an optimal test point traversing schedule.
- Traversing the compressor map, one speed-line at a time, is a relatively fast

method. However, a little can be gained if one traverses the map optimally by jumping between different speed-lines.

- System identification methods can be used to estimate heat and efficiency parameters prior to the turbocharger measurements.

5.2 Future Work

A natural progression is to adapt the optimal control method to the closed loop gas stand, but it can be used for other systems as well, which may or may not include the turbocharger. For example, for some types of after-treatment testing, a steady-state exhaust temperature is needed. If an optimal control suitable engine model is added to the turbocharger, the same principle can be applied to solve this problem.

Bibliography

Joel Andersson. *A General-Purpose Software Framework for Dynamic Optimization*. PhD thesis, Arenberg Doctoral School, KU Leuven, Department of Electrical Engineering (ESAT/SCD) and Optimization in Engineering Center, Kasteelpark Arenberg 10, 3001-Heverlee, Belgium, October 2013. Cited on pages 3 and 21.

ASME. PTC 10-1997, Performance test code on compressors and exhausters. American Society of Mechanical Engineers, New York, 1997. Cited on page 2.

Jonas Asprion, Oscar Chinellato, and Lino Guzzella. Optimal control of diesel engines: Numerical methods, applications, and experimental validation. *Mathematical Problems in Engineering*, 2014. Cited on page 3.

Nick Baines, Karl D. Wygant, and Antonis Dris. The analysis of heat transfer in automotive turbochargers. *Journal of Engineering for Gas Turbines and Power*, 2010. Cited on pages 3 and 12.

Mikael Bengtsson. A control-oriented 0D model of a turbocharger gas stand including heat transfer. Master's thesis, Linköpings universitet, SE-581 83 Linköping, 2015. Cited on page 3.

Moritz Diehl. Numerical optimal control. 2011. Cited on page 3.

Kristoffer Ekberg. Effects of non ideal inlet and outlet pipes on measured compressor efficiency. Master's thesis, Linköpings universitet, SE-581 83 Linköping, 2015. Cited on page 3.

Lars Eriksson. Modeling and control of turbocharged SI and DI engines. *Oil & Gas Science and Technology - Rev. IFP*, 62(4):523–538, 2007. Cited on page 2.

Lars Eriksson and Lars Nielsen. *Modeling and Control of Engines and Drivelines*. John Wiley & Sons, 2014. Cited on pages 2, 8, and 11.

Joseph Kirk. *Traveling Salesman Problem - Genetic Algorithm*. MathWorks - MATLAB Central File Exchange, 2014. Cited on page 31.

Viktor Leek. An optimal control toolbox for MATLAB based on casADi. Master's thesis, Linköping University, SE-581 83 Linköping, 2016. Cited on page 3.

Viktor Leek, Kristoffer Ekberg, and Lars Eriksson. Development and usage of a continuously differentiable heavy duty diesel engine model equipped with VGT and EGR. In *SAE 2017 World Congress & Exhibition*, number SAE Technical Paper 2017-01-0611, Detroit, United States, April 2017. Cited on page 3.

Oskar Leufvén and Lars Eriksson. A surge and choke capable compressor flow model - validation and extrapolation capability. *Control Engineering Practice*, 21(12):1871–1883, 2013. Cited on page 8.

Xavier Llamas and Lars Eriksson. Parameterizing compact and extensible compressor models using orthogonal distance minimization. *Journal of Engineering for Gas Turbines and Power*, 139(1), 2016. Cited on pages 2, 8, and 9.

Xavier Llamas and Lars Eriksson. Control-oriented compressor model with adiabatic efficiency extrapolation. In *SAE 2017 World Congress & Exhibition*, number SAE Technical Paper 2017-01-1032, Detroit, MI, USA, April 2017. Cited on pages 2, 8, 9, and 10.

Xavier Llamas and Lars Eriksson. LiU CPgui: A toolbox for parameterizing compressor models. Technical Report LiTH-ISY-R-3102, Department of Electrical Engineering, Linköpings Universitet, SE-581 83 Linköping, Sweden, 2018. Cited on pages 2 and 8.

P. Olmeda, V Dolz, F. Arnau, and M.A Reyes-Belmonte. Determination of heat flows inside turbochargers by means of a one dimensional lumped model. *Mathematical and Computer Modelling*, 2011. Cited on page 3.

SAE. SAE J1826 – Turbocharger Gas Stand Test Code. SAE standard, 1995a. Cited on page 2.

SAE. SAE J922 – Turbocharger Nomenclature and Terminology. SAE standard, 1995b. Cited on page 2.

J. Serrano, P. Olmeda, F. Arnau, and A. Dombrovsky. General procedure for the determination of heat transfer properties in small automotive turbochargers. *International Journal of Engines*, 2014. Cited on page 3.

Martin Sivertsson and Lars Eriksson. Modeling for optimal control: A validated diesel-electric powertrain model. In *SIMS 2014 - 55th International Conference on Simulation and Modelling*, Aalborg, Denmark, 2014. Cited on page 3.

Eric Stemler and Patrick Lawless. The design and operation of a turbocharger test facility designed for transient simulation. 1997. Cited on page 2.

TOMLAB. *PROPT - Matlab Optimal Control Software*. `http://www.tomdyn.com/`, 2016. Cited on page 3.

G. Venson, J. Barros, and J. Pereira. Development of an automotive turbocharger test stand using hot gas. In *SAE Brasil Congress and Exhibit*, Brasil, January 2006. Cited on page 2.

N. Watson and M.S. Janota. *Turbocharging the Internal Combustion Engine*. The Macmillan Press ltd, 1982. ISBN 0-333-24290-4. Cited on page 8.

A. Wächter. *A General-Purpose Software Framework for Dynamic Optimization*. PhD thesis, Arenberg Doctoral School, KU Leuven, Department of Electrical Engineering (ESAT/SCD) and Optimization in Engineering Center, Kasteelpark Arenberg 10, 3001-Heverlee, Belgium, October 2013. Cited on pages 3 and 21.

M. Young and D. Penz. The design of a new turbocharger test facility. In *SAE International Congress and Exposition*, Detroit, United States, February 1990. Cited on page 2.